

80x71mm (300 x 300 DPI)

Apigenin Restrains Colon Cancer Cell Proliferation via Targetedly Blocking the PKM2-dependent Glycolysis

Shuhua **Shan**^{†§}, Jiangying **Shi**[†], Peng **Yang**[†], Bin **Jia**^{†▽}, Haili **Wu**[†], Xiaoli **Zhang**[†], Zhuoyu **Li**^{†,‡,*}

[†]Key Laboratory of Chemical Biology and Molecular Engineering of National Ministry of Education, Institute of Biotechnology, Shanxi University, Taiyuan, China

[‡]School of Life Science and Technology, Shanxi University, Taiyuan, China

[§]Department of Biology, Taiyuan Normal University, Taiyuan, China

[▽]School of Basic Medical Science, Shanxi Medical University, Taiyuan, China

***Corresponding Author:** Zhuoyu Li. Tel: +86 351 7018268. Fax: +86 351 7018268. Email:

lzy@sxu.edu.cn

ABSTRACT:

Apigenin (AP), as an anti-cancer agent, has been widely explored. However, the molecular targets of apigenin on tumor metabolism are unclear. Currently, we found that AP could block the cellular glycolysis through restraining the tumor-specific pyruvate kinase M2 (PKM2) activity and expression, and further significantly induce the anti-colon cancer effects. The IC_{50} values of AP against HCT116, HT29 and DLD1 cells respectively were 27.9 ± 2.45 , 48.2 ± 3.01 and 89.5 ± 4.89 μ M. Fluorescence spectra and solid-phase AP extraction assays proved that AP could directly bind to PKM2 and markedly inhibit PKM2 activity in vitro and in HCT116 cells. Interestingly, in the presence of D-fructose-1, 6-diphosphate (FBP), the inhibitory effect of AP on PKM2 had not been reversed, which suggests AP is a new allosteric inhibitor of PKM2. Meantime, RT-PCR and western blot assays showed that AP could ensure a low PKM2/PKM1 ratio in HCT116 cells via blocking β -catenin/c-Myc/PTBP1 signal pathway. Hence, PKM2 represents a novel potential target of AP against colon cancer.

KEY WORDS: Apigenin (AP); Colon cancer cells; Pyruvate kinase M2 (PKM2); Glycolysis; Cell proliferation

28 1. Introduction

29 Apigenin (AP), 4', 5, 7-trihydroxyflavone, a well-known flavonoid compound, is
30 generally found in various dietary plant foods, such as celery, thyme, celeriac, chamomile,
31 onions, orange and tea et al (Zheng et al. 2005). Apigenin has significantly exhibited
32 anti-tumor activity in various kinds of cancer cells, including colon cancer ^{1, 2}, lung cancer ³,
33 prostate cancer cells ⁴, pancreatic cancer ⁵, hepatocarcinogenesis and breast cancer ⁶. AP
34 inhibits the proliferation of tumor cells through coordinating multiple survival-related
35 pathways, including PI3K/Akt/NF- κ B ⁷, Wnt/ β -catenin ⁸, insulin-like growth factor ⁹, mTOR
36 signaling pathway et al ¹⁰. Nonetheless, the potential targets of AP-induced anti-tumor effects
37 and its impact on tumor metabolism have not been investigated.

38 As everyone knows that Warburg effect is a metabolic characteristic of cancer cells.
39 Even in the case of adequate oxygen, tumor cells prefer to convert glucose into lactate instead
40 of complete oxidation via Krebs cycle ¹¹. Hence, glycolysis is the major pathway for energy
41 generation of tumor cells, and is crucial for the cancer cell proliferation and survival ¹².
42 Pyruvate kinase (PK)-catalyzed reaction is the final rate-limiting step of glycolysis ¹³.
43 Mammalian cells have two PK genes: PKM1 and PKM2 are encoded by one PK gene, while
44 PKL and PKR are encoded by another gene ¹⁴. Most tumor cells uniformly express PKM2,
45 thereby PKM2 plays a pivotal role in the cancer progression as a key regulator of the Warburg
46 effect ¹⁵. Hence, screening drugs which targeting inhibit PKM2 activity and expression is a
47 potentially novel strategy for anticancer therapy. In previous studies, some inhibitors of
48 PKM2 have been found, but few of them have selective.

49 In this study, we firstly found that AP exhibited anti-colon cancer effects through blocking
50 the glycolysis pathway of PKM2-mediated. Further, fluorescence spectra and solid-phase AP
51 extraction assays showed that AP could selectively bind to PKM2 and further suppress PKM2
52 activity in vitro and in HCT116 cells, but not PKM1. Fructose 1, 6-bisphosphate (FBP), an
53 intermediate metabolite of glycolysis, is an allosteric effector of PKM2, and can allosterically
54 activate the PKM2 activity ¹⁶. Interestingly, the restraining effect of AP on PKM2 had not been

reversed by FBP, which hints AP is a new allosteric inhibitor of PKM2. Meantime, AP also could negatively regulate the PKM2/PKM1 ratio via blocking the β -catenin/c-Myc/PTBP1 signal pathway. Hence, our results suggest that PKM2 represents a novel potential target of AP against colon cancer.

2. Materials and methods

2.1 Chemicals and antibodies

RPMI-1640, DMEM/F12 (1:1) medium and fetal bovine serum (FBS) were purchased from GIBCO, Inc (GrandIsland, NY, USA). Apigenin (AP), D-fructose-1, 6-diphosphate (FBP), Glucose, oligomycin, 2-deoxy-D-glucose (2-DG) and Lithium (LiCl) were purchased from Sigma-Aldrich, Inc (St. Louis, MO, USA). Antibodies for PKM1 and PKM2 were obtained from Cell Signaling Technology, Inc (Danvers, MA, USA). Antibodies for β -catenin, Glu1 and c-Myc were obtained from Bioworld Technology, Inc (Minneapolis, MN, USA); Glucose Test Kit was obtained from Biovision, Inc (Mountain View, CA). Lactate Assay Kit, ATP Assay Kit and Glutaminase Test Kit were obtained from Nanjing Jiancheng Biotechnology Co., Ltd (Nanjing, China). GAPDH antibody was purchased from Abmart, Inc (Arlington, MA, USA); PTBP1 antibody was purchased from Sangon Biotechnology (Shanghai, China); Human Recombinant PKM2 (Re-PKM2) and PKM1 (Re-PKM1) were purified by our laboratory.

2.2 Cell culture

Human colon cancer cell lines (HCT116, HT29 and DLD1) were purchased from the Chinese Type Culture Collection (Shanghai China). The cell culture method was described in our previous study¹⁷.

2.3 Cell survival assay

MTT assay was performed according to our previously described method with some modifications¹⁷. Apigenin was dissolved in dimethylsulfoxide (DMSO). HCT116, HT29 and DLD1 cells were incubated with the different concentration of AP (0, 10, 20, 40, 60 μ M) for 24 h. Next, cells were incubated for 4 h by 5 mg/ml MTT (Sigma), and then 150 μ l DMSO

(Sigma) were added to cell medium. The absorbance at 570 nm was measured. Cell survival rate was calculated with the formula: cell survival rate (%) = $\text{OD}_{570} \text{ AP-treated} / \text{OD}_{570} \text{ control} \times 100 \%$.

2.4 Colony-formation assay

HCT116, HT29 and DLD1 cells were treated with 0, 15, 30 μM AP for 7 d respectively, and next the cell colonies were fixed, stained and photographed as the previously described method¹⁸. Colony formation rate was counted with the formula: colony formation rate % = $(\text{Clones} / \text{Seeded Cells}) \times 100 \%$.

2.5 Measurement of Glucose consumption, lactate production and ATP contents

HCT116 cells were incubated in 6-well plates (1×10^5 cells/ per well) overnight. Then these cells were subsequently treated with the different concentration of AP (0, 10, 20, 40 μM) for 24h. The contents of glucose and lactate in culture medium were determined with Glucose Test Kit (Biovision) and Lactate Assay Kit (Nanjing Jiancheng Bioengineering, Nanjing China) individually. The cells were broken by the ultrasound. Then cell supernatant was obtained by centrifuging at 6,000 rpm for 10 min and used to determine the ATP contents with ATP Assay Kit (Jiancheng Bioengineering).

2.6 Determination of extracellular acidification rates (ECAR)

HCT116 cells were inoculated into XF24-well culture plate which was obtained from Seahorse Bioscience (North Billerica, MA, USA) at density 1×10^4 cells/well and were subsequently intervened for 24 h with the different doses of AP (0, 20, 40 μM) after cells attachment. Cells were washed for two times and incubated for 1 h in the 37 °C non- CO_2 incubator in 500 μl XF Base Medium DMEM (356mg/l L-glutamine, pH 7.45). ECAR was determined after the successive injection of 10 mM glucose, 1 μM oligomycin and 50 mM 2-DG at the indicated times. Seahorse XF24 Extracellular Analyzer was run using 3 cycles of

107 3 min mixing, 2 min waiting, and 3 min measurement. The data of ECAR (mpH/min) was
108 recorded simultaneously.

109 **2.7 Determination of Pyruvate Kinase Activity**

110 PKM2 activity was measured as the previous method with some modifications ^{13, 14}.
111 Enzymatic reactive mixture contained 50 mM Tris-HCl buffer (pH 7.5), 0.5 mM
112 phosphoenolpyruvic acid (PEP), 100 mM KCl, 180 μ M NADH, 2 mM adenosine
113 5-diphosphate (ADP), 10 mM $MgCl_2$, 8 U/ml of LDH and 20–100 ng re-PKM2. AP was
114 dissolved in DMSO. FBP was dissolved in ddH₂O to the proper concentration. In the vitro
115 inhibition experiment, the suitable AP or DMSO solution and 10 ng/ μ l of re-PKM2 were
116 mixed and pre-incubated for 30 min at 37 °C. Then the suitable FBP or DMSO solution was
117 added to the above mixture and sequentially incubated for 30 min. Re-PKM2 activity was
118 measured and counted in the absence or presence of 125 μ M FBP according to the previously
119 described method ¹⁴. PKM2 activity was defined as the quantity of β -nicotinamide adenine
120 dinucleotide (NADH) oxidized by 1 mg of re-PKM2 per minute. Re-PKM1 activity was
121 determined as above described method.

122 HCT116 cells were inoculated into 6-well culture plate (1×10^5 cells/well) overnight and
123 were subsequently treated with the different concentration of AP (0, 10, 20, 40 μ M) for 24 h.
124 Then, these cells were broken and centrifuged at 6,000 rpm for 10 min and the supernatant
125 was used to determine the PKM2 activity as above described method.

126 **2.8 Fluorescence Spectra Measurements**

127 Pyruvate Kinase was dissolved in phosphate buffer saline (PBS), and the final
128 concentration was 4.3×10^{-7} M. AP was dissolved in DMSO. A solution of 1.0 ml of Pyruvate
129 Kinase was titrated with AP of different concentration and the reaction mixture incubated for
130 3 min at different temperature (25 °C, 30 °C, 37 °C, 42 °C) respectively before the
131 measurements. Fluorescence spectra of Pyruvate Kinase and Pyruvate Kinase-AP mixture
132 were recorded from 315 to 400 nm. Excitation and emission slits were set as 10 nm.
133 Fluorescence spectra were recorded with an excitation of 295 nm.

134 **2.9 Solid-phase extraction assay**

135 Solid-phase extraction assay was performed as described previously with some
136 modifications ¹⁴. HCT116 cell lysate (2 mg protein) was mixed with AP (6 mg), and the
137 mixture revolved overnight at 4 °C and removed the supernatant by centrifugation. The
138 precipitate of crystal AP with bound cellular protein was washed for three times with chilled
139 buffer (50 mM Tris-HCl, pH 7.5, 2 mM EDTA, 150 mM NaCl, 1 mM NaF, 10 % glycerol)
140 followed by dissolving and boiling in SDS-PAGE loading buffer for 5 min. The samples were
141 separated by 10 % SDS-polyacrylamide gel and next transferred to polyvinylidene fluoride
142 (PVDF) membrane, followed by incubation with PKM2 primary and secondary antibodies.
143 The protein band of PKM2 was visualized by enhanced chemoluminescence.

144 **2.10 Real-time PCR assay**

145 Real-time PCR assay was carried out according to described previously method with some
146 modifications ¹⁹. Total RNA of HCT116 cells by control or AP-treated was extracted with
147 Trizol reagent and then reversely transcribed to cDNA by PrimeScript RT Master Mix. The
148 relative expression of each targeted gene in RNA level was determined by Real-time PCR
149 assay.

150 **2.11 Western blot assay**

151 Western blot assay was executed according to our previously described method ¹⁷. HCT116
152 cells were treated as above 2.5 described for 24 h. Cells were degraded using the cell lysis
153 buffer and incubated for 30 min on ice, followed by centrifuging for 15 min at 13,000 rpm.
154 The equal protein was separated by SDS-PAGE assay and next transferred to PVDF
155 membrane, followed by incubation with primary and secondary antibodies. The relative
156 expression of each target protein was visualized with enhanced chemiluminescence.

157 **2.12 Small interfering RNA (siRNA) transfection assay**

158 A siRNA against β -catenin (sense 5'-GGAUGUGGAUACCUCCCAATT-3', antisense
159 5'-UUGGGAGGUAUCCACAUCCTT-3') and a negative control siRNA (sense
160 5'-UUCUCCGAACGUGUCACGUTT-3', anti-sense, 5'-ACGUGACACGUUC GGA GAA

161 TT-3') were obtained from Genepharma (Shanghai China), HCT116 cells were inoculated
162 into 6-well culture plate overnight and next were transiently transfected with 10 nM of siRNA
163 using HiPerFect Transfection Reagent (QIAGEN) as the manufacturer's instructions. The
164 β -catenin knockdown was determined by qRT-PCR and western blot assays 48 h
165 post-transfection.

166 **2.13 Statistical Analysis**

167 Statistical significance was measured with SPSS 17.0 software. Data were statistically
168 analyzed using one-way analysis of variance, followed by Tukey's post-hoc test. Results were
169 represented as the mean \pm standard deviation (SD). The P-values of less than 0.05 ($p<0.05$)
170 and 0.01 ($p<0.01$) were indicated that the difference was significant and extremely significant
171 compared with the control.

172 **3 Results**

173 **3.1 AP significantly restrains colon cancer cell survival and colony formation**

174 To explore AP-induced anti-colon cancer effects, we determined the effects of AP on
175 survival and colony-formation ability of HCT116, HT29 and DLD1 cells. The results
176 manifested that the survival ratios of three colon cancer cell lines (HCT116, HT29 and DLD1)
177 showed a remarkably dose-dependent reduction with AP treatment, and further the viability
178 rates of HCT116, HT29 and DLD1 cells were 35 %, 44 % and 66 % with 60 μ M AP for 24 h.
179 (Figure 1C). The IC₅₀ values of AP against HCT116, HT29, and DLD1 cells respectively were
180 27.9 \pm 2.45, 48.2 \pm 3.01, and 89.5 \pm 4.89 μ M. Furthermore, as shown in Figure 1 A and B, AP
181 treatment also could significantly decrease the colony sizes and numbers of HCT116, HT29
182 and DLD1 cells compared to the control group. These results suggest that AP inhibits
183 markedly colon cancer cell proliferation, and further prove that the inhibition rate of AP on
184 HCT116 cell is highest compared with HT29 and DLD1 cells. Therefore, HCT116 cell line
185 was selected for further experiments.

186 **3.2 AP induces the blockage of glycolysis in HCT116 cells**

187 The glycolysis and glutamine metabolism are the major metabolic pathways for cancer

cell survival and proliferation. To investigate whether AP affected the metabolic rates of HCT116 cells, the relevant key indicators were measured. The results showed that AP significantly inhibited the glycolytic rate in HCT116 cells, as manifested by cellular lactate production and glucose consumption (Figure 2C and D), while the glutaminase activity had no effect after AP treatment (Figure 2G). Extracellular acidification rate (ECAR) from proton production rate represents a direct indicator of glycolytic capacity. Seahorse XF24 Extracellular Analyzers revealed that AP treatment could significantly reduce the glycolysis, glycolytic capacity and glycolytic reserve of HCT116 cell (Figure 2 E and F). Meantime, AP treatment also could seal off the expression of the glucose transporter-1(Glu1) in mRNA and protein levels (Figure 2A and B). As expected, the blockage of glycolysis by AP-induced led to the decrease of ATP contents in HCT116 cells (Figure 2H). These results indicate that AP can display the anti-proliferative effects in colon cancer through reducing the rate of cellular glycolysis.

3.3 AP exists the interaction With Re-PKM2 in vitro

To investigate whether the interaction exists between AP and re-PKM2, the effect of AP on fluorescence spectra of PKM2 were measured. As shown in Figure 3, fluorescence intensity of PKM2 was quenched obviously (near 340 nm) in the presence of AP at room temperature. The types of fluorescence quenching contain static and dynamic quenching. Dynamic quenching gives the credit to the collisions between two fluorescent luminophors, whereas static quenching results from the formation of a new non fluorescent complex^{20, 21}. The dynamic quenching constant (K_{sv}) increases along with the rise of temperature and rate constant (K_q) is lower than $2.0 \times 10^{10} \text{ (L} \cdot \text{mol}^{-1} \cdot \text{S}^{-1})$ in the process of dynamic quenching, but the case is the opposite in the process of static quenching in accordance with the fluorescence quenching theory²¹. As shown in table 1, K_{sv} values were reduced gradually with the elevation of temperature (25 °C, 30 °C, 37 °C, 42 °C) and K_q was greater than $2.0 \times 10^{10} \text{ (L} \cdot \text{mol}^{-1} \cdot \text{S}^{-1})$, which indicates the fluorescence quenching of PKM2 by AP-induced is a static quenching through forming a new complex.

Further, we confirmed the interaction manner between AP and PKM2 by the values of binding constants (K_A) and binding sites (n). As shown in table 2, the number of binding site (n) was approximately one at 25 °C, 30 °C, 37 °C, 42 °C, which suggested that the temperature changes had little effect on the binding of AP and PKM2. The main interaction manners between a small molecule and a protein molecule have several types, including hydrogen bonding, hydrophobic interaction, electrostatic attraction, vander waals force et al²². The relative changes of entropy (ΔS) and enthalpy (ΔH) values can evaluate the types of the main interaction. Specifically, when $\Delta H > 0$ and $\Delta S > 0$, hydrophobic force is the main force²². According to our results, the value of ΔG was negative for the AP, while their ΔH and ΔS were positive, which means that the direct interaction between PKM2 and AP is a spontaneous process along with entropy increasing, and further is driven mainly by hydrophobic force (Table. 3).

3.4 AP can allosterically inhibit the PKM2 activity in vitro

The PKM1 and PKM2 are originated from a PKM gene transcript through alternative splicing, in which 21 residues are different²³. PKM1 exhibits high constitutive enzymatic activity, while PKM2 is less active and has allosteric effect²⁴. Our results showed that AP could inhibit PKM2 activity (Figure 4A) and the inhibitory effect of AP on re-PKM2 was dose-dependent and selective, whereas AP could did not affect re-PKM1 activity in vitro (Figure 4C). According to the literature, the glycolytic metabolite FBP is an allosteric activator of PKM2²⁵. To confirm whether AP could allosterically regulate PKM2 activity, re-PKM2 activity was measured in the presence or absence of FBP. The results showed that re-PKM2 had not been activated in the presence of AP by FBP, which suggests that there is the same site for AP and FBP binding to PKM2 (Figure 4B). In other words, PKM2 activity can be allosterically inhibited by AP in vitro.

3.5 PKM2 is a potential target protein of AP in HCT116 cells

To confirm whether AP could bind to intracellular PKM2 in HCT116, we extracted cellular proteins binding to AP in HCT116 lysates by solid-phase assay. SDS-PAGE

combined with western blotting analysis revealed that PKM2 was a target protein of AP (Figure 5A and B). Further, AP also could inhibit PKM2 activity in a dose-dependent manner in HCT116 cells (Figure 5C). Subsequently, the effect of AP on PKM2 activity was determined in the presence of FBP. As expected, the inhibitory effect of AP on PKM2 activity had not been reversed by FBP (Figure 5D), which further confirms that AP is a new allosteric inhibitor of PKM2.

3.6 AP decreases the expression of PKM2 in HCT116 by blocking the β -catenin/c-Myc /PTBP1 pathway

To investigate whether AP could affect the expression of PKM2, the RT-PCR and western blot assays were performed. The results showed that AP treatment could significantly decrease the RNA and protein levels of PKM2 in a dose-dependent manner, whereas the PKM1 expression in mRNA level was markedly increased and had not change in protein level (Figure 6 A and B). Polypyrimidine Tract Binding Protein (PTBP1), a pivotal regulator of PKM splicing, which selectively promotes PKM2 splicing²⁶. Minami et al study²⁷ showed that c-Myc could positively regulate PTBP1 expression in bladder cancer cells. Our results found that AP treatment effectively reduced the PTBP1, β -catenin and c-Myc expression in a dose-dependent manner in mRNA and protein levels in HCT116 cells (Figure 6 C and D).

Lithium (LiCl), an inhibitor of GSK-3 β , is known to activate the wnt/ β -catenin pathway and its downstream target gene c-Myc expression by preventing β -catenin degradation²⁸. Therefore, to further confirm whether the inhibitory effect of AP on PKM2 expression was mediated by wnt/ β -catenin pathway, the addition of LiCl mimicked the β -catenin over-expression. The cells were pretreated for 24 h with 10 mM LiCl, and then treated with 40 μ M AP for 24 h. As shown in Figure 6E, LiCl treatment markedly increased β -catenin expression, and further the inhibitory effects of AP on β -catenin, c-Myc, PTBP1 and PKM2 expression were obviously reversed after LiCl pretreatment, and whereas the knockdown of β -catenin by siRNA had the opposite effect (Figure 6F and G). These results indicate that the inhibitory effect of AP on PKM2 expression is realized via blocking the

269 β -catenin/c-Myc/PTBP1 pathway in HCT116 cells.

270 **4 Discussion**

271 Previous studies have demonstrated that apigenin, as an edible plant-derived flavonoid,
272 can induce markedly anti-colon cancer effects via modulating several signaling pathways,
273 including inhibition of the AKT and ERK ¹, supersession of autophagy formation ², activation
274 of caspase cascade pathway ²⁹, induction of G2/M cell-cycle arrest ³⁰. In present, we also
275 found that AP significantly suppressed HCT116, HT29 and DLD1 cells survival in a
276 dose-dependent manner and the inhibitory effects of AP on three cell lines had obviously
277 difference (Figure 1).

278 As shown in Figure 1 C, HCT116 displayed the highest responsive rate to AP compared
279 to other two colon cancer cell lines (HT29 and DLD1). Duke's classification for colorectal
280 cancer is a widely applied classification system and represents the malignancy of colon cancer
281 ³¹. It is reported that HCT116, HT29 and DLD1 cell lines are typical representative of Duke's
282 type A, B and C in human colon cancer cell lines ^{31, 32}, indicates that the malignant degree of
283 HCT116 cell is the lowest compared with HT29 and DLD1 cell lines. Furthermore, it is
284 generally known that the wild type p53, as a tumor suppressor gene, has a profound effect on
285 inhibiting cancer development, whereas mutant p53 plays an opposite role. The studies
286 showed that HCT116 cell line harbored the wild type p53, while DLD1 and HT29 cell lines
287 were mutant p53^{33, 34}. Therefore, the highest inhibitory effect of AP on HCT116 cell
288 proliferation may owe to its lower malignant degree and P53 gene types.

289 Further, we found that AP could induce a switch of glycolytic cancer cells, and result in
290 the decrease of colon cancer cells survival (Figure 2). Previous studies proved that different
291 from normal cells, cancer cells preferentially take glycolysis for supplying the distinct
292 metabolic needs of cell proliferation, even in the abundance of oxygen. Therefore, aerobic
293 glycolysis or the Warburg effects is the main way in which tumor cells get energy and is
294 pivotal for the survival and growth of cancer cells. Our results firstly demonstrated that in
295 HCT116 cells, AP not only blocked the cellular intake of glucose, but also decreased glucose

296 consumption and lactate production, which further led to the decrease of ATP contents
297 (Figure 2). The results prove that the anti-proliferative effects of AP on colon cancer cells
298 partly give the credit to the blockage of glycolysis.

299 PKM2 is the last rate-limiting enzyme in glycolysis, which catalyzed from
300 phosphoenolpyruvate (PEP) to pyruvate^{35, 36}. Lots of evidences showed that PKM2 was a key
301 regulator for glucose metabolism and played an important role in colon cancer progression^{37, 38,}
302 ³⁹. Therefore, development of selectively targeting PKM2 inhibitors for cancer therapy
303 remains an optimal strategy. PKM2 is highly homologous to PKM1 and they have the same
304 catalytic site. However, PKM2 contains a unique allosteric regulatory site, making it possible to
305 screen selectively inhibitor of targeting the allosteric site of PKM2. Previous study showed that
306 PKM2 enzyme activity was strongly inhibited by apigenin in vitro⁴⁰. In present study, we
307 found that apigenin not only in vitro could significantly inhibit the activity of PKM2 (Figure
308 4A), and importantly it also could play the same effect in HCT116 cell (Figure 5C), but not
309 the PKM1 (Figure 4C). Further, our results manifested that apigenin displayed the inhibitory
310 effects of PKM2 through directly binding to PKM2 (Figure 3 and Figure 4). FBP is an
311 allosteric activator of PKM2⁴¹. Our results showed that PKM2 inhibition by AP-induced in
312 vitro and in lysates of HCT116 cell is not reversed by FBP, and further speculates that apigenin
313 specifically targets at the allosteric FBP binding site of PKM2 (Figure 4B and Figure 5D).
314 Hence, these results indicate apigenin probably is a new allosteric inhibitor of PKM2.

315 Furthermore, our results also demonstrated that apigenin selectively blocked the expression
316 of PKM2 in mRNA level, but induced the PKM1 expression in HCT116 cell, which indicates
317 that apigenin maybe involves in the alternative splicing of PKM pre-Mrna (Figure 6 A and B).
318 Previous studies demonstrated that c-Myc, an oncogenic transcription factor, is one of the
319 target genes in the downstream of β -catenin⁴², which can ensure a high PKM2/PKM1 ratio by
320 up-regulating transcription of PTBP, hnRNPA1 and hnRNPA2⁴³. As expectedly, we found
321 that apigenin significantly reduced the expression of β -catenin and its downstream target gene
322 c-Myc and PTBP1, and the β -catenin overexpression by LiCl-mimicked could partly reverse

the effects (Figure 6). Therefore, we speculate that the inhibitory effects of PKM2 expression by apigenin-induced partly attribute to β -catenin/c-Myc/PTBP1-mediated alternative splicing event.

In conclusion, apigenin targeting at PKM2-mediated glycolysis pathway plays a crucial role in inhibition of colon cancer cell proliferation (Figure 7). Further, apigenin mainly induces a switch of glycolysis in colon cells through blocking the activity and expression of PKM2. Mechanically, apigenin can bind to the allosteric site of PKM2 to inhibit the PKM2 activity; Interestingly, apigenin also selectively inhibits the PKM2 expression by blocking the β -catenin/c-Myc/PTBP1 signal pathway. The study shed light on the key role of apigenin in cancer metabolic reprogramming.

Fundings

This study was supported by the National Natural Science Foundation of China (No. 31500630, 31770382), Shanxi Scholarship Council of China (No. 2015-2), Shanxi Province Science Foundation for Youths (No. 2015021200), Scientific and Technological Innovation Programs of Higher Education Institutions in Shanxi (No. 2015175), National Training Program of Innovation and Entrepreneurship for Undergraduates (No. 201610119005).

Notes

The authors declare no conflict of interest.

Figure legends

Figure 1. Effects of AP on colon cancer cell survival. (A) Cell colony-formation ability was observed using Stereoscopic microscope. Cells were treated with 0, 15, 30 μ M AP for 7 d. (B) Clone-formation rate was determined by crystal violet. (C) Cell viability ratio was measured using MTT assay. HCT116, HT29 and DLD1 cells were treated with the increasing concentration of AP (0, 10, 20, 40, 60 μ M) for 24 h. * p <0.05, ** p <0.01 versus control.

350 **Figure 2. AP induces the blockage of glycolysis in HCT116 cells.** (A, B) Effect of AP on
351 Glu-1 expression in mRNA (A) and protein (B) levels. HCT-116 cells were treated with 0, 10,
352 20, 40 μ M AP for 24 h. (C, D, G) Effects of AP on glucose consumption (C), lactase
353 production (D) and glutaminase activity (G). Cells were treated as Figure. 2 A described. (E, F)
354 Effects of AP on extracellular acidification rate (ECAR). HCT-116 cells were intervened with
355 0, 20, 40 μ M AP for 24 h. ECAR was determined after the sequential injection of 10 mM
356 glucose, 1 μ M oligomycin and 50 mM 2-DG at the indicated times. (H) Effect of AP on ATP
357 contents in HCT116 cells. Cells were intervened as Figure. 2 A described. * p <0.05 and **
358 p <0.01 vs. control group.

359 **Figure 3. Effect of AP on fluorescence spectra of PKM2.** λ_{ex} = 295 nm,
360 [Apigenin]= 7.5×10^{-4} M, curves 1–11 pH 7.4, at room temperate. Apigenin increased as the
361 direction of the arrow. PKM2, pyruvate kinase-2.

362 **Figure 4. Effects of AP on the re-PKM2 and re-PKM1 activities in vitro.** (A) Effect of
363 AP on re-PKM2 activity. (B) The inhibitory effect of AP on re-PKM2 activity in the presence
364 of 125 μ M FBP. The mixture of re-PKM2 and AP pre-incubated at 37 °C for 30 min, and
365 then the mixture which was added FBP persistently incubated at same temperture for 30 min.
366 PK activity was calculated by measuring the change of absorbance at 340 nm from 0 to 8 min.
367 * p <0.05, ** p <0.01 vs. control. FBP, D-fructose-1, 6-bisphosphate. (C) Effect of AP on the
368 re-PKM1 activity.

369 **Figure 5. The target protein bound to AP is identified by solid-phase and western**
370 **blotting assays.** (A) Cellular proteins by solid-phase AP-extracted were showed by
371 SDS-PAGE in HCT116 cells. (B) The target protein bound to AP was identified by western
372 blotting assay. (C) Effect of AP on PKM2 activity in HCT116 cells. Cells were treated as
373 Figure. 2 A described and used the cell lysates to determine the activity of PKM2. (D) Effect
374 of AP on PKM2 activity in HCT116 cells in the presence or absence of FBP. After cells were
375 treated by 40 μ M AP, the cell lysate incubated with 125 μ M FBP for 30 min at 37 °C to
376 determine the activity of PKM2. ** p <0.01 vs. control.

377 **Figure 6. AP inhibits PKM2 expression by blocking the β -catenin/c-Myc/PTBP1**
378 **pathway.** (A) Effects of AP treatment on the PKM1 and PKM2 expressions in mRNA (A) and
379 protein (B) levels were measured by RT-PCR and western blotting assays. Cells were treated
380 as Figure. 2 (A) described. (C, D) Effects of AP on the β -catenin, c-Myc and PTBP1
381 expressions in mRNA (C) and protein (D) levels. (E, F) Effects of β -catenin siRNA on the
382 expression levels of β -catenin, c-Myc, PKM2 and PKM1. HCT116 cells were transfected
383 using β -catenin siRNA or negative control (NC) siRNA for 48 h. (G) Effects of LiCl on the
384 inhibitory levels of β -catenin, c-Myc, PKM2 and PTBP1 by AP-induced. HCT116 cells were
385 pretreated with 10 mM LiCl for 24 h and next intervened with 40 μ M AP for 24 h. * p <0.05,
386 ** p <0.01 vs. control.

387 **Figure 7. AP restrains colon cancer cell proliferation via targetedly blocking the**
388 **PKM2-dependent glycolysis.**

389

390

391

392

393

394

395

396

397

398

399

400

401

402

403

404 **References**

- 405 1. Shao, H.; Jing, K.; Mahmoud, E.; Huang, H.; Fang, X.; Yu, C. Apigenin sensitizes colon
406 cancer cells to antitumor activity of ABT-263. *Mol Cancer Ther* **2013**, *12*, 2640-50.
- 407 2. Lee, Y.; Sung, B.; Kang, Y. J.; Kim, D. H.; Jang, J. Y.; Hwang, S. Y.; Kim, M.; Lim, H.
408 S.; Yoon, J. H.; Chung, H. Y.; Kim, N. D. Apigenin-induced apoptosis is enhanced by
409 inhibition of autophagy formation in HCT116 human colon cancer cells. *Int J Oncol* **2014**, *44*,
410 1599-606.
- 411 3. Pan, X.; Yang, Z.; Zhou, S.; Zhang, H.; Zang, L. Effect of apigenin on proliferation and
412 apoptosis of human lung cancer NCI-H460 cells. *J Southern Med Univ* **2013**, *33*, 1137-40.
- 413 4. Shukla, S.; Bhaskaran, N.; Babcook, M. A.; Fu, P.; MacLennan, G. T.; Gupta, S. Apigenin
414 inhibits prostate cancer progression in TRAMP mice via targeting PI3K/Akt/FoxO pathway.
415 *Carcinogenesis* **2014**, *35*, 452-60.
- 416 5. Johnson, J. L.; de Mejia, E. G. Flavonoid apigenin modified gene expression associated
417 with inflammation and cancer and induced apoptosis in human pancreatic cancer cells through
418 inhibition of GSK-3 β /NF- κ B signaling cascade. *Mol Nutr Food Res* **2013**, *57*,
419 2112-27.
- 420 6. Huang, C.; Wei, Y. X.; Shen, M. C.; Tu, Y. H.; Wang, C. C.; Huang, H. C. Chrysin
421 abundant in *morinda citrifolia* fruit water-EtOAc extracts, combined with apigenin
422 synergistically induced apoptosis and inhibited migration in human breast and liver cancer
423 cells. *J Agr Food Chem* **2016**, *64*, 4235-45.
- 424 7. Erdogan, S.; Doganlar, O.; Doganlar, Z. B.; Serttas, R.; Turkecul, K.; Dibirdik, I.; Bilir,
425 A. The flavonoid apigenin reduces prostate cancer CD44⁺ stem cell survival and migration
426 through PI3K/Akt/NF- κ B signaling. *Life Sci* **2016**, *162*, 77-86.
- 427 8. Xu, M.; Wang, S.; Song, Y. U.; Yao, J.; Huang, K.; Zhu, X. Apigenin suppresses
428 colorectal cancer cell proliferation, migration and invasion via inhibition of the
429 Wnt/ β -catenin signaling pathway. *Oncol Lett* **2016**, *11*, 3075-3080.
- 430 9. Babcook, M. A.; Gupta, S. Apigenin modulates insulin-like growth factor axis:

431 implications for prevention and therapy of prostate cancer. *Curr Drug Targets* **2012**, 1-14.

432 10. Bridgeman, B. B.; Wang, P.; Ye, B.; Pelling, J. C.; Volpert, O. V.; Tong, X. Inhibition of
433 mTOR by apigenin in UVB-irradiated keratinocytes: A new implication of skin cancer
434 prevention. *Cell Signal* **2016**, 28, 460-8.

435 11. Warburg, O.; Wind, F.; Negelein, E. The metabolism of tumors in the body. *Journal Gen*
436 *Physiol* **1927**, 8, 519-30.

437 12. Vander Heiden, M. G.; Cantley, L. C.; Thompson, C. B. Understanding the warburg
438 effect: The metabolic requirements of cell proliferation. *Science* **2009**, 324, 1029-33.

439 13. Christofk, H. R.; Vander Heiden, M. G.; Harris, M. H.; Ramanathan, A.; Gerszten, R. E.;
440 Wei, R.; Fleming, M. D.; Schreiber, S. L.; Cantley, L. C. The M2 splice isoform of pyruvate
441 kinase is important for cancer metabolism and tumour growth. *Nature* **2008**, 452, 230-3.

442 14. Chen, J.; Xie, J.; Jiang, Z.; Wang, B.; Wang, Y.; Hu, X. Shikonin and its analogs inhibit
443 cancer cell glycolysis by targeting tumor pyruvate kinase-M2. *Oncogene* **2011**, 30, 4297-306.

444 15. Li, Z.; Yang, P. The multifaceted regulation and functions of PKM2 in tumor progression.
445 *Biochim Biophys Acta* **2014**, 1846, 285-96.

446 16. Dombrackas, J. D.; Santarsiero, B. D.; Mesecar, A. D. Structural basis for tumor
447 pyruvate kinase M2 allosteric regulation and catalysis. *Biochemistry* **2005**, 44, 9417-29.

448 17. Shan, S.; Li, Z.; Newton, I. P.; Zhao, C.; Guo, M. A novel protein extracted from foxtail
449 millet bran displays anti-carcinogenic effects in human colon cancer cells. *Toxicol Lett* **2014**,
450 227, 129-38.

451 18. Shan, S.; Shi, J.; Li, Z.; Gao, H.; Shi, T. Targeted anti-colon cancer activities of a millet
452 bran-derived peroxidase were mediated by elevated ROS generation. *Food Funct* **2015**, 6,
453 2331-8.

454 19. Li, Z.; Zhang, L.; Zhao, Y.; Li, H.; Xiao, H.; Fu, R.; Zhao, C.; Wu, H. Cell-surface
455 GRP78 facilitates colorectal cancer cell migration and invasion. *Int J Biochem Cell Biol* **2013**,
456 45, 987-94.

457 20. Li, Y. Q.; Zhou, F. C.; Gao, F.; Bian, J. S.; Shan, F. Comparative evaluation of quercetin,

458 isoquercetin and rutin as inhibitors of alpha-glucosidase. *J Agr Food Chem* **2009**, 57,
459 11463-8.

460 21. Vella, F. Principles of bioinorganic chemistry. *Biochem Educ* **1995**, 23, 115.

461 22. Ross, P. D.; Subramanian, S. Thermodynamics of protein association reactions-forced
462 contributing to stability. *Biochemistry* **1981**, 20, 3096-3102.

463 23. Anastasiou, D.; Yu, Y.; Israelsen, W. J.; Jiang, J. K.; Boxer, M. B.; Hong, B. S.; Tempel,
464 W.; Dimov, S.; Shen, M.; Jha, A.; Yang, H.; Mattaini, K. R.; Metallo, C. M.; Fiske, B. P.;
465 Courtney, K. D.; Malstrom, S.; Khan, T. M.; Kung, C.; Skoumbourdis, A. P.; Veith, H.;
466 Southall, N.; Walsh, M. J.; Brimacombe, K. R.; Leister, W.; Lunt, S. Y.; Johnson, Z. R.; Yen,
467 K. E.; Kunii, K.; Davidson, S. M.; Christofk, H. R.; Austin, C. P.; Inglese, J.; Harris, M. H.;
468 Asara, J. M.; Stephanopoulos, G.; Salituro, F. G.; Jin, S.; Dang, L.; Auld, D. S.; Park, H. W.;
469 Cantley, L. C.; Thomas, C. J.; Vander Heiden, M. G. Pyruvate kinase M2 activators promote
470 tetramer formation and suppress tumorigenesis. *Nat Chem Biol* **2012**, 8, 839-47.

471 24. Ikeda, Y.; Noguchi, T. Allosteric regulation of pyruvate kinase M2 isozyme involves a
472 cysteine residue in the intersubunit contact. *J biol chem* **1998**, 273, 12227-33.

473 25. Ikeda, Y.; Tanaka, T.; Noguchi, T. Conversion of non-allosteric pyruvate kinase isozyme
474 into an allosteric enzyme by a single amino acid substitution. *J biol chem* **1997**, 272,
475 20495-501.

476 26. Calabretta, S.; Bielli, P.; Passacantilli, I.; Piloizzi, E.; Fendrich, V.; Capurso, G.; Fave, G.
477 D.; Sette, C., Modulation of PKM alternative splicing by PTBP1 promotes gemcitabine
478 resistance in pancreatic cancer cells. *Oncogene* **2016**, 35, 2031-9.

479 27. Minami, K.; Taniguchi, K.; Sugito, N.; Kuranaga, Y.; Inamoto, T.; Takahara, K.; Takai, T.;
480 Yoshikawa, Y.; Kiyama, S.; Akao, Y., MiR-145 negatively regulates Warburg effect by
481 silencing KLF4 and PTBP1 in bladder cancer cells. *Oncotarget* **2017**, 8, 33064-33077.

482 28. Hedgepeth, C. M.; Conrad, L. J.; Zhang, J.; Huang, H. C.; Lee, V. M. Y.; Klein, P. S.,
483 Activation of the Wnt Signaling Pathway: A Molecular Mechanism for Lithium Action. *Dev*
484 *Biol* **1997**, 185, 82-91.

- 485 29. Turktekin, M.; Konac, E.; Onen, H. I.; Alp, E.; Yilmaz, A.; Menevse, S. Evaluation of the
486 effects of the flavonoid apigenin on apoptotic pathway gene expression on the colon cancer
487 cell line (HT29). *J Med Food* **2011**, *14*, 1107-17.
- 488 30. Wang, W.; VanAlstyne, P. C.; Irons, K. A.; Chen, S.; Stewart, J. W.; Birt, D. F. Individual
489 and interactive effects of apigenin analogs on G2/M cell-cycle arrest in human colon
490 carcinoma cell lines. *Nutr Cancer* **2004**, *48*, 106-14.
- 491 31. Ehrig, K.; Kilinc, M. O.; Chen, N. G.; Stritzker, J.; Buckel, L.; Zhang, Q.; Szalay, A. A.,
492 Growth inhibition of different human colorectal cancer xenografts after a single intravenous
493 injection of oncolytic vaccinia virus GLV-1h68. *J Transl Med* **2013**, *11*, 1-15.
- 494 32. Hittlet, A.; Legendre, H.; Nagy, N.; Bronckart, Y.; Pector, J. C.; Salmon, I.; Yeaton, P.;
495 Gabius, H. J.; Kiss, R.; Camby, I., Upregulation of galectins-1 and -3 in human colon cancer
496 and their role in regulating cell migration. *Int J Cancer* **2003**, *103*, 370-9.
- 497 33. Bao, C. M.; Da-Peng, B. I.; Zhou, D. M.; Of, D.; Second, T.; Effect of tumor necrosis
498 factor alpha on mutant p53 protein expression in colorectal cancer cell lines. *Chinese Journal*
499 *of Current Advances in General Surgery* **2011**, *11*, 17-19.
- 500 34. He, K.; Zheng, X.; Zhang, L.; Yu, J., Hsp90 inhibitors promote p53-dependent apoptosis
501 through PUMA and Bax. *Mol cancer ther* **2013**, *12*, 2559-68.
- 502 35. Warburg, O. On the origin of cancer cells. *Science* **1956**, *123*, 309-14.
- 503 36. Hsu, P. P.; Sabatini, D. M. Cancer Cell Metabolism: Warburg and Beyond. *Cell* **2008**,
504 *134*, 703-7.
- 505 37. Li, Z.; Yang, P.; Li, Z. The multifaceted regulation and functions of PKM2 in tumor
506 progression. *Biochim Biophys Acta* **2014**, *1846*, 285-296.
- 507 38. Yang, P.; Li, Z.; Wang, Y.; Zhang, L.; Wu, H. Secreted pyruvate kinase M2 facilitates cell
508 migration via PI3K/Akt and Wnt/ β -catenin pathway in colon cancer cells. *Biochem Bioph Res*
509 *Co* **2015**, *459*, 327-332.
- 510 39. Spoden, G. A.; Rostek, U.; Lechner, S.; Mitterberger, M.; Mazurek, S.; Zwerschke, W.
511 Pyruvate kinase isoenzyme M2 is a glycolytic sensor differentially regulating cell

512 proliferation, cell size and apoptotic cell death dependent on glucose supply. *Exp Cell Res*
513 **2009**, *315*, 2765-74.

514 40. Aslan, E.; Adem, S. In vitro effects of some flavones on human pyruvate kinase
515 isoenzyme M2. *J Biochem Mol Toxicol* **2015**, *29*, 109-113.

516 41. Jurica, M. S.; Mesecar, A.; Heath, P. J.; Shi, W.; Nowak, T.; Stoddard, B. L. The allosteric
517 regulation of pyruvate kinase by fructose-1,6-bisphosphate. *Structure* **1998**, *6*, 195-210.

518 42. Noubissi, F. K.; Elcheva, I.; Bhatia, N.; Shakoori, A.; Ougolkov, A.; Liu, J.; Minamoto,
519 T.; Ross, J.; Fuchs, S. Y.; Spiegelman, V. S. CRD-BP mediates stabilization of betaTrCP1 and
520 c-myc mRNA in response to beta-catenin signalling. *Nature* **2006**, *441*, 898-901.

521 43. David, C. J.; Chen, M.; Assanah, M.; Canoll, P.; Manley, J. L. HnRNP proteins controlled
522 by c-Myc deregulate pyruvate kinase mRNA splicing in cancer. *Nature* **2010**, *463*, 364-8.

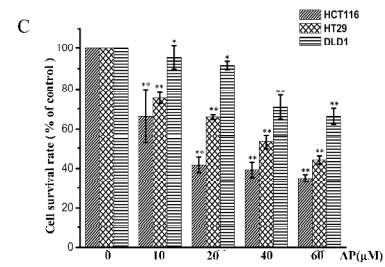
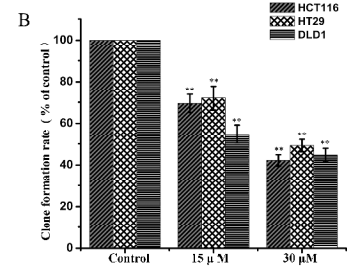
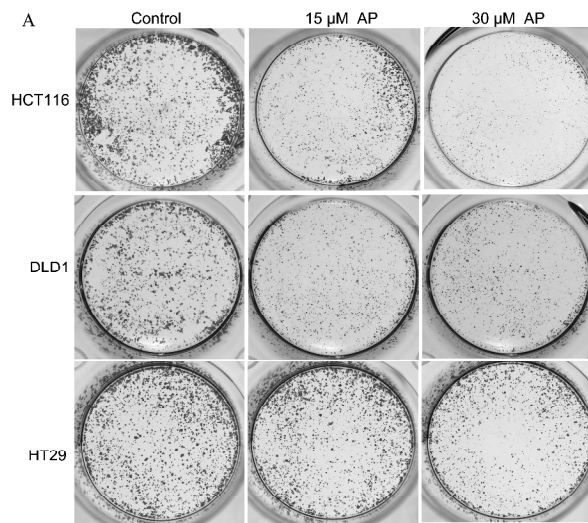
523

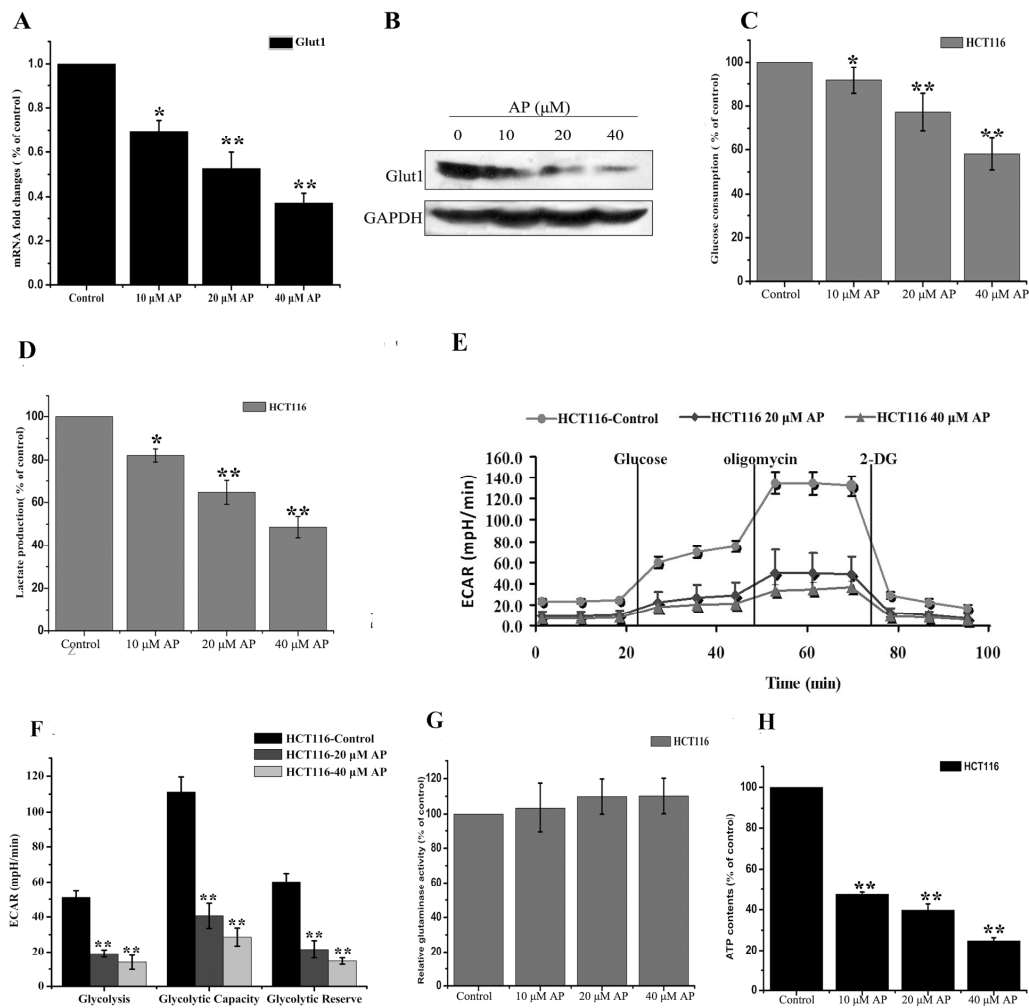
524

525

526

527





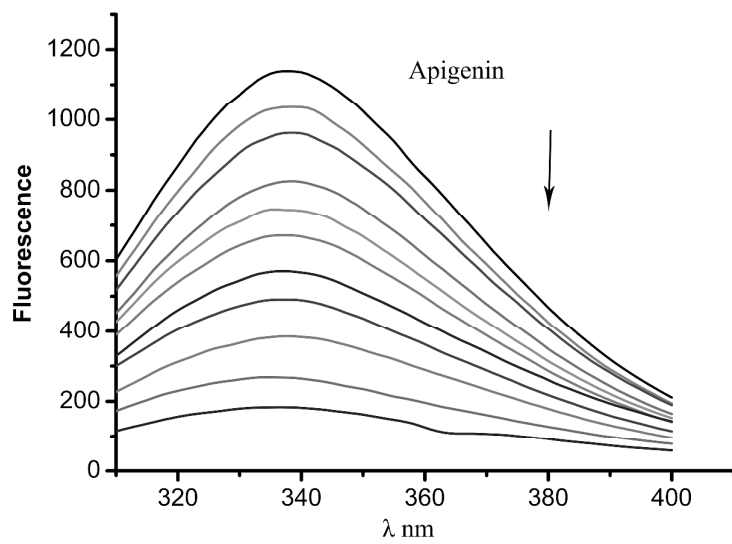


Table 1 Stern–Volmer quenching constant values of the interactions between AP and PKM2

T(°C)	$K_{sv}/10^5$ (L·mol ⁻¹)	$K_q/10^{13}$ (L·mol ⁻¹ ·S ⁻¹)	R ²
25	2.41	2.41	0.99
30	2.30	2.30	0.99
37	2.29	2.29	0.99
42	1.87	1.87	0.99

Table 2 Values of K_A and n of the interaction between AP and PKM2

T(°C)	$K_A/10^5$ (L·mol ⁻¹)	n	R ²
25	2.80	1.02	0.99
30	3.30	1.05	0.99
37	7.26	1.11	0.99
42	9.95	1.12	0.99

Table 3 Thermodynamic of interaction between AP and PKM2

T(°C)	ΔG (kJ·mol ⁻¹)	ΔH (kJ·mol ⁻¹)	ΔS (J·mol ⁻¹ K ⁻¹)
25	-31.1	62.7	314
30	-32.0		
37	-34.8		
42	-36.2		

